J Mater Sci (2008) 43:6734–6746
DOI 10.1007/s10853-008-2784-x

Effects of environment on creep behavior of two oxide/oxide ceramic–matrix composites at 1200 °C

M. B. Ruggles-Wrenn · P. Koutsoukos · S. S. Baek

Received: 18 March 2008 / Accepted: 6 June 2008 / Published online: 9 August 2008

Abstract The tensile creep behavior of two oxide/oxide ceramic–matrix composites (CMCs) was investigated at 1200 °C in laboratory air, in steam, and in argon. The composites consist of a porous oxide matrix reinforced with laminated, woven mullite/alumina (Nextel^{TM}720) fibers, have no interface between the fiber and matrix, and rely on the porous matrix for flaw tolerance. The matrix materials were alumina and aluminosilicate. The tensile stress–strain behavior was investigated and the tensile properties were measured at 1200 °C. Tensile creep behavior of both CMCs was examined for creep stresses in the 80–150 MPa range. Creep run-out defined as 100 h at creep stress was achieved in air and in argon for stress levels $\leq$100 MPa for both composites. The retained strength and modulus of all specimens that achieved run-out were evaluated. The presence of steam accelerated creep rates and reduced creep life of both CMCs. In the case of the composite with the aluminosilicate matrix, no-load exposure in steam at 1200 °C caused severe degradation of tensile strength. Composite microstructure, as well as damage and failure mechanisms were investigated. Poor creep performance of both composites in steam is attributed to the degradation of the fibers and densification of the matrix. Results indicate that the aluminosilicate matrix is considerably more susceptible to densification and coarsening of the porosity than the alumina matrix.

Introduction

Advances in aerospace propulsion technologies have raised the demand for structural materials that have superior long-term mechanical properties and retained properties under high temperature, high pressure, and varying environmental factors, such as moisture [1]. Ceramic–matrix composites (CMCs) capable of maintaining excellent strength and fracture toughness at high temperatures are prime candidate materials for such aerospace applications. Additionally, the lower densities of CMCs and their higher use temperatures, together with a reduced need for cooling air, allow for improved high-temperature performance when compared to conventional nickel-based superalloys [2]. Concurrent efforts in optimization of the CMCs and in design of the combustion chamber are expected to accelerate the insertion of the CMCs into aerospace turbine engine applications, such as combustor walls [3–5]. Because these applications require exposure to oxidizing environments, the thermodynamic stability and oxidation resistance of CMCs are vital issues. The need for environmentally stable composites motivated the development of CMCs based on environmentally stable oxide constituents [6–11].

The main advantage of CMCs over monolithic ceramics is their superior toughness, tolerance to the presence of cracks and defects, and non-catastrophic mode of failure. It is widely accepted that to avoid brittle fracture behavior in CMCs and improve the damage tolerance, a weak fiber/matrix interface is needed, which serves to deflect matrix cracks and to allow subsequent fiber pullout [12–14]. It has

The views expressed are those of the authors and do not reflect the official policy or position of the United States Air Force, Department of Defense or the U.S. Government.

M. B. Ruggles-Wrenn (✉) · P. Koutsoukos
Department of Aeronautics and Astronautics, Air Force Institute of Technology, Wright-Patterson Air Force Base, OH 45433-7765, USA
e-mail: marina.ruggles-wrenn@afit.edu

S. S. Baek
Agency for Defense Development, Daejeon, South Korea

been demonstrated that similar crack-deflecting behavior can also be achieved by means of a finely distributed porosity in the matrix instead of a separate interface between matrix and fibers [15]. This microstructural design philosophy implicitly accepts the strong fiber/matrix interface. The concept has been successfully demonstrated for oxide/oxide composites [6, 9, 11, 16, 17]. Resulting oxide/oxide CMCs exhibit damage tolerance combined with inherent oxidation resistance. An extensive review of the mechanisms and mechanical properties of porous-matrix CMCs is given in [18, 19].

Porous-matrix oxide/oxide CMCs exhibit several behavior trends that are distinctly different from those exhibited by traditional CMCs with a fiber–matrix interface. Most SiC-fiber-containing CMCs exhibit longer life under static loading and shorter life under cyclic loading [20]. For these materials, fatigue is significantly more damaging than creep. Zawada et al. [21] examined the high-temperature mechanical behavior of a porous matrix Nextel^{TM}610/aluminosilicate composite. Results revealed excellent fatigue performance at 1000 °C, the material exhibited high fatigue limit, long fatigue life, and near 100% strength retention. Conversely, creep lives were short, indicating low creep resistance and limiting the use of that CMC to temperatures below 1000 °C.

Because creep is shown to be considerably more damaging to porous-matrix oxide/oxide CMCs [21, 22], creep testing is well suited for assessing the long-term durability and high-temperature performance of the oxide/oxide ceramic composites with porous matrix. The objective of this study is to investigate the effects of environment on high-temperature creep performance of two oxide/oxide CMCs, consisting of a porous oxide matrix reinforced with woven mullite/alumina (Nextel^{TM}720) fibers: Nextel^{TM}720/alumina and Nextel^{TM}720/aluminosilicate. Creep-rupture tests of each composite were conducted at 1200 °C in air, argon, and steam environments for creep stresses ranging from 80 to 150 MPa. Resulting creep performance imposes limitations on the use of these materials in high-temperature applications. The composite microstructure, as well as damage and failure mechanisms are discussed.

Experimental procedure

Material

The two materials studied were Nextel^{TM}720/Alumina (N720/A) and Nextel^{TM}720/aluminosilicate (N720/AS), commercially available oxide/oxide ceramic composites (COI Ceramics, San Diego, CA), consisting of a porous oxide matrix reinforced with Nextel^{TM}720 fibers. Each composite was supplied in a form of 305 × 305 mm^2 plates comprised of 12 0°/90° woven layers. The N720/A plates were 2.8 mm thick, with a density of ~2.77 g/cm^3, fiber volume of approximately 45%, and matrix porosity of ~24%. The N720/AS plates were 2.6 mm thick with a density of ~2.68 g/cm^3, fiber volume of approximately 48%, and matrix porosity of ~22%. Both composites were manufactured using the same processing techniques. The fiber fabric was infiltrated with the matrix in a sol–gel process. The laminate was dried with a "vacuum bag" technique under low pressure and low temperature, then pressureless sintered [23]. No coating was applied to the fibers. The damage tolerance of the N720/A and N720/AS composites is enabled by a porous matrix. Representative micrograph of the untested N720/A material is presented in Fig. 1, which shows 0° and 90° fiber tows as well as numerous matrix cracks. In the case of the as-processed material, most are shrinkage cracks formed during processing rather than matrix cracks generated during loading. The untested N720/AS material exhibits similar microstructural features.

Mechanical testing

A servocontrolled MTS mechanical testing machine equipped with hydraulic water-cooled collet grips, a compact two-zone resistance-heated furnace, and two temperature controllers

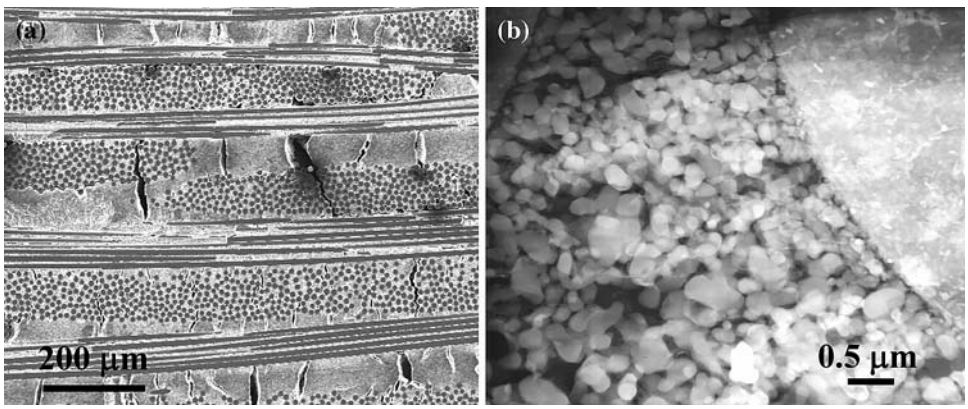

Fig. 1 As-received N720/A ceramic composite: (**a**) Overview and (**b**) Porous nature of the matrix is evident

was used in all tests. An MTS TestStar II digital controller was employed for input signal generation and data acquisition. Strain measurement was accomplished with an MTS high-temperature air-cooled uniaxial extensometer of 12.5 mm gage length. Tests in steam environment employed an alumina susceptor (tube with end caps), which fits inside the furnace. The specimen gage section is located inside the susceptor, with the ends of the specimen passing through slots in the susceptor. Steam is introduced into the susceptor (through a feeding tube) in a continuous stream with a slightly positive pressure, expelling the dry air and creating a near 100% steam environment inside the susceptor. An alumina susceptor was also used in tests conducted in argon environment. In this case high-purity argon was introduced into the susceptor creating an inert gas environment around the test section of the specimen. For elevated temperature testing, two S-type thermocouples were bonded to the specimen using alumina cement (Zircar) to calibrate the furnace on a periodic basis. The furnace controllers (using non-contacting S-type thermocouples exposed to the ambient environment near the test specimen) were adjusted to determine the power settings needed to achieve the desired temperature of the test specimen. The determined power settings were then used in actual tests. The power settings for testing in steam were determined by placing the specimen instrumented with two S-type thermocouples in steam environment and repeating the furnace calibration procedure. To calibrate the furnace for testing in argon, the specimen instrumented with two S-type thermocouples was placed in argon environment.

All tests were performed at 1200 °C. In all tests, a specimen was heated to test temperature in 25 min, and held at temperature for additional 15 min prior to testing. Dog bone-shaped specimens of 152 mm total length with a 10-mm-wide gage section were used in all tests. All N720/A test specimens used in this study were cut from a single plate. Likewise all N720/AS specimens were cut from a single plate. Tensile tests were performed in stroke control with a constant displacement rate of 0.05 mm/s in laboratory air. Creep-rupture tests were conducted in load control in accordance with the procedure in ASTM standard C 1337 in laboratory air, steam, and argon. In all creep tests the specimens were loaded to the creep stress level at the stress rate of 15 MPa/s. Creep run-out was defined as 100 h at a given creep stress. In each test, stress–strain data were recorded during the loading to the creep stress level and the actual creep period. Thus both total strain and creep strain could be calculated and examined. To determine the retained tensile strength and modulus, specimens that achieved run-out were subjected to tensile test to failure at 1200 °C. In some cases one specimen was tested per test condition. The authors recognize that this is a limited set of data; however, extreme care was taken in generating the data. Selective duplicate tests have demonstrated the data to be very repeatable. This exploratory effort serves to identify the behavioral trends and to determine whether a more rigorous investigation should be undertaken.

Fracture surfaces of failed specimens were examined using SEM (FEI Quanta 200 HV) as well as an optical microscope (Zeiss Discovery V12). The SEM specimens were carbon coated.

Results and discussion

Monotonic tension

Tensile results obtained for N720/A and N720/AS composites at 1200 °C were consistent with those reported earlier [22, 24] (COI Ceramics, unpublished data). For the N720/A composite, the average ultimate tensile strength (UTS) was 192 MPa, elastic modulus, 75 GPa, and failure strain, 0.38%. For the N720/AS composite, the average UTS was 230 MPa, elastic modulus, 65 GPa, and failure strain, 0.44%. It is worthy of note that in all tension tests, as well as in all other tests reported below, the failure occurred within the gage section of the extensometer.

Creep rupture

Results of the creep-rupture tests for N720/A and N720/AS composites are summarized in Table 1, where creep strain accumulation and rupture time are shown for each creep stress level and test environment. Creep curves obtained in air, argon, and steam are shown in Figs. 2–4, respectively. Results from prior work [22] are included in Table 1 and in Figs. 2 and 4 for comparison.

All creep curves obtained for the N720/A composite at 1200 °C in air environment (Fig. 2a) exhibit primary and secondary creep regimes. Transition from primary to secondary creep occurs early in creep life. At the stress of 80 MPa, primary creep transitions to secondary creep after $\sim$10 h. At stresses $\geq$100 MPa, primary creep persists for not more than 4 h. Secondary creep continues to failure. Likewise, creep curves obtained for N720/AS (Fig. 2b) exhibit primary and secondary creep regimes. Unlike N720/A, the N720/AS composite transitions from primary to secondary creep somewhat later in creep life. At stresses of 100 and 125 MPa, primary creep persists during the first 20 h of the creep test. For both composites, creep strain increases as the applied stress increases from 80 to 100 MPa (125 MPa in the case of N720/AS), then decreases with increasing stress. At a given stress, the N720/A composite accumulates larger creep strain than N720/AS. For N720/A CMC, all creep strains accumulated in air significantly exceed the failure strain obtained in the tension test. In the case of N720/AS composite, all creep

Table 1 Summary of creep–rupture results for the N720/A and N720/AS ceramic composites at 1200 °C, in laboratory air, in argon, and in steam

Test environment	Creep stress (MPa)	Creep strain (%)	Time to rupture (h)
N720/A			
Air	80	0.59	100[b]
Air[a]	100	1.52	41.0
Air[a]	125	1.28	18.1
Air[a]	150	0.58	0.27
Argon	80	0.66	100[b]
Argon	100	0.96	100[b]
Argon	125	1.89	36.3
Argon	150	0.33	0.88
Steam[a]	80	2.96	46.0
Steam[a]	100	1.41	2.49
Steam[a]	125	0.90	0.24
Steam[a]	150	0.40	0.03
N720/AS			
Air	80	0.26	100[b]
Air	100	0.40	100[b]
Air	125	0.59	29.5
Air	150	0.53	10.0
Argon	80	0.36	100[b]
Argon	100	0.49	100[b]
Argon	125	0.39	1.77
Argon	150	0.61	1.45
Steam	80	0.79	10.9
Steam	100	0.36	0.27
Steam	125	0.58	0.20

[a] Data from Ruggles-Wrenn et al. [22]

[b] Run-out

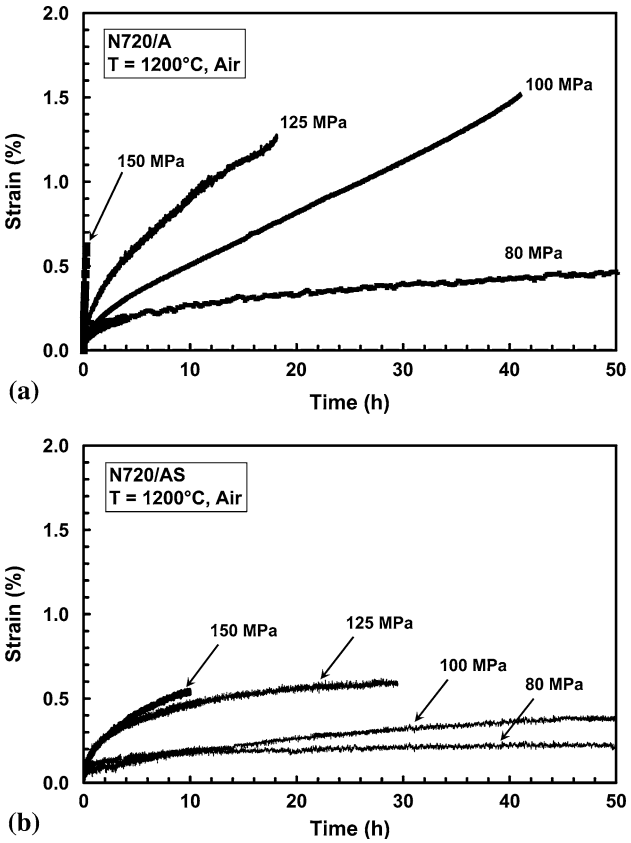

Fig. 2 Creep strain vs. time curves at 1200 °C in laboratory air for: (**a**) N720/A, data from Ruggles-Wrenn et al. [22] and (**b**) N720/AS

strains accumulated in air are <0.6%. Furthermore, only the creep strains accumulated at stresses ≥125 MPa exceed the failure strain produced in the tension test. It is important to recognize that the total strain incurred in a creep-rupture test represents a sum of two contributions: (1) that due to the initial loading up to the specific creep stress level, and (2) that accumulated during the actual creep period. For the N720/A specimens tested at creep stresses ≤125 MPa, close to 90% of total strain was accumulated during the creep period. However, for the N720/A specimen tested at 150 MPa, creep strain accounted only for 33% of the total strain. In the case of all N720/AS specimens tested in air creep strain represents ~70% of the total strain, regardless of the creep stress level.

Results in Figs. 3 and 4 reveal that test environment has little influence on the appearance of the creep curves obtained for both N720/A and N720/AS composites. The creep curves produced by each composite in argon and in steam are qualitatively similar to the creep curves obtained for that material in air. Furthermore, the creep strains accumulated by each composite in argon are comparable to those accumulated by that CMC in air. In contrast, the presence of steam had a noticeable effect on creep strain and creep lifetime of both CMCs. At 80 MPa, specimens of both composites tested in steam accumulated significantly more creep strain than the specimens tested in air. In the case of N720/A, creep strain produced at 80 MPa in steam was five times that produced in air. For N720/AS, creep strain accumulated at 80 MPa in steam was three times that obtained in air. While both composites survived 100 h of creep at 80 MPa in air and at 100 MPa in argon, neither CMC achieved creep run-out in steam. Moreover, N720/AS was not subjected to creep at 150 MPa in steam because several N720/AS specimens failed before reaching the 150 MPa stress level. Apparently exposure to steam environment during 25 min of heating to 1200 °C followed by a 15 min hold at 1200 °C significantly degraded the tensile strength of N720/AS. To explore the effect of short-term no-load exposure to steam on tensile properties of N720/AS, additional specimens were aged for 12 h at 1200 °C in steam then tested in tension to failure. Results are discussed below. Note that such no-load exposure at

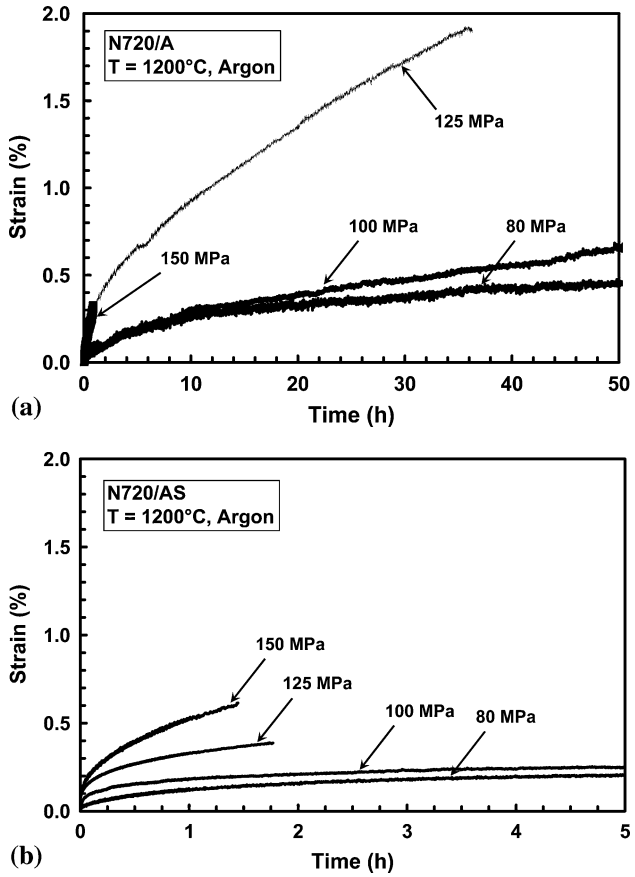

Fig. 3 Creep strain vs. time curves at 1200 °C in argon for: (**a**) N720/A and (**b**) N720/AS

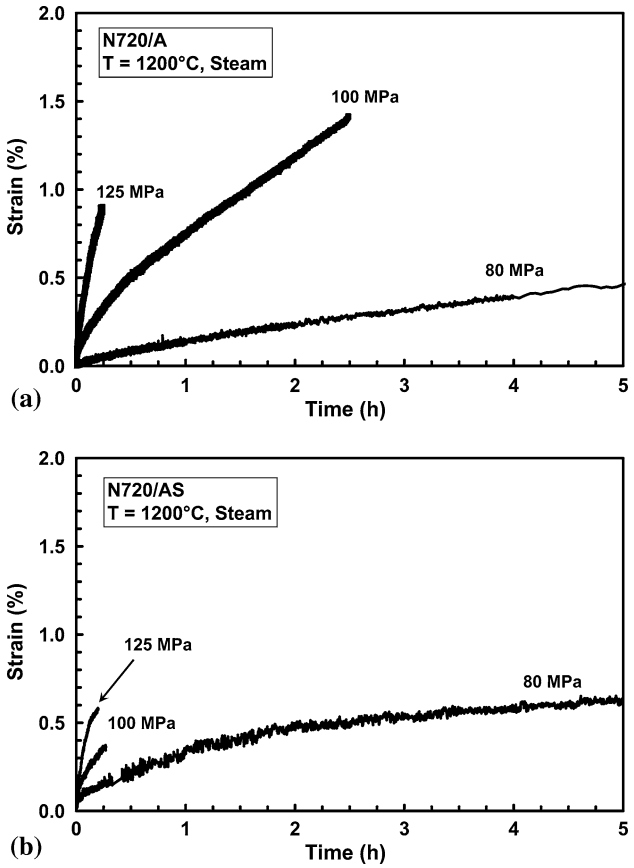

Fig. 4 Creep strain vs. time curves at 1200 °C in steam for: (**a**) N720/A, data from Ruggles-Wrenn et al. [22] and (**b**) N720/AS

1200 °C in steam was shown to have no effect on tensile strength of N720/A composite [25].

Minimum creep rate was reached in all tests. Creep rate as a function of applied stress is presented in Fig. 5, where results obtained in air and in steam for N720/A composite from prior work [22] are included for comparison. In air the secondary creep rate of N720/A can be as high as 100 times that of the N720/AS CMC. In argon and in steam, the N720/A creep rate can be as high as 10 times the N720/AS rate. For both composites, the minimum creep rate increases by approximately two orders of magnitude as the creep stress increases from 80 to 150 MPa. For a given creep stress, the N720/A creep rate in argon is close to that in air, while the creep rate in steam is approximately an order of magnitude higher than that in air. In the case of N720/AS composite, creep rate in argon is approximately one order of magnitude higher and creep rate in steam, nearly two orders or magnitude higher, than the creep rate obtained in air for a given stress.

Stress–rupture behavior is summarized in Fig. 6, where results for N720/A composite in air and in steam from prior work [22] are also included. As expected, creep life decreases with increasing applied stress for both composites. In the case of the N720/A composite, the presence of argon was beneficial. The increase in creep lifetimes due to argon was at least twofold for applied stress levels $\geq$100 MPa. On the contrary, the presence of steam dramatically reduced creep lifetimes. The reduction in creep life due to steam was at least 90% for applied stress levels $\geq$100 MPa, and 54% for the applied stress of 80 MPa. In the case of N720/AS, the presence of argon has little effect on the creep lifetimes (up to 100 h) for applied stresses $\leq$100 MPa. For stresses $\geq$125 MPa, creep lifetimes were reduced by as much as an order of magnitude in the presence of argon. An even greater degradation of creep life is seen in the presence of steam. The loss of creep life due to steam was $\sim$99% for applied stress levels $\geq$100 MPa, and 90% at 80 MPa.

Retained strength and modulus of the specimens that achieved a run-out are summarized in Table 2. Tensile stress–strain curves obtained for the specimens subjected to prior creep are presented in Fig. 7 together with the tensile stress–strain curves for the as-processed material. The N720/A composite subjected to 100 h of prior creep at 80 MPa in air retained over 90% of its tensile strength; the modulus loss was limited to 14%. The N720/A specimens pre-crept in argon

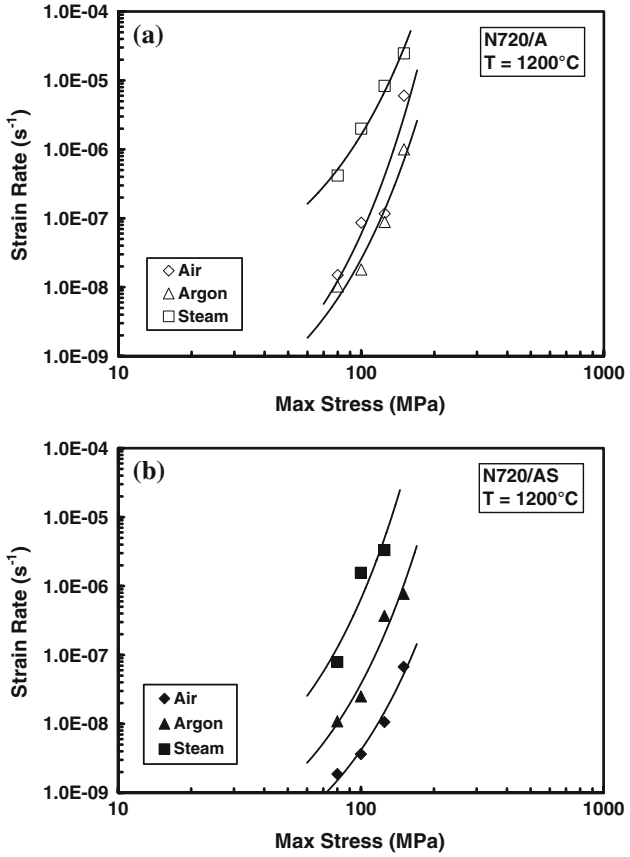

Fig. 5 Minimum creep rate as a function of applied stress at 1200 °C in laboratory air, in argon, and in steam for: (**a**) N720/A and (**b**) N720/AS. Data for N720/A in air and in steam from Ruggles-Wrenn et al. [22] are also shown

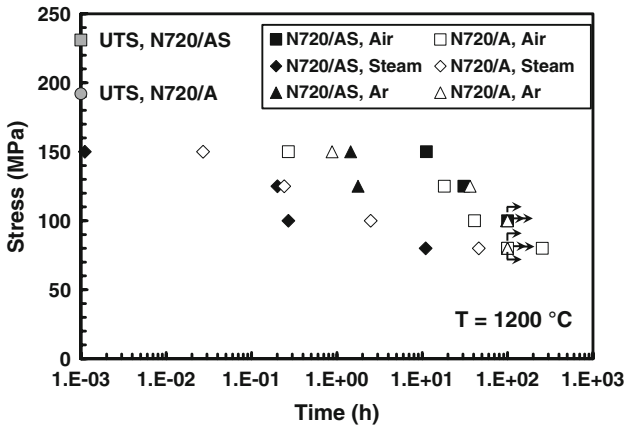

Fig. 6 Creep stress vs. time to rupture for N720/A and N720/AS ceramic composites at 1200 °C in laboratory air, in argon, and in steam. Data for N720/A in air and in steam from Ruggles-Wrenn et al. [22] are also shown

Table 2 Retained properties of the N720/A and N720/AS specimens subjected to prior creep at 1200 °C in laboratory air and in argon environments

Environment	Creep stress (MPa)	Retained strength (MPa)	Retained modulus (GPa)	Strain at failure (%)
N720/A				
Air	80	174	64.5	0.31
Argon	80	180	54.7	0.38
Argon	100	161	53.8	0.31
N720/AS				
Air	80	116	65.6	0.18
Air	100	97.1	55.3	0.19
Argon	80	105	65.1	0.15
Argon	100	87.0	49.0	0.17

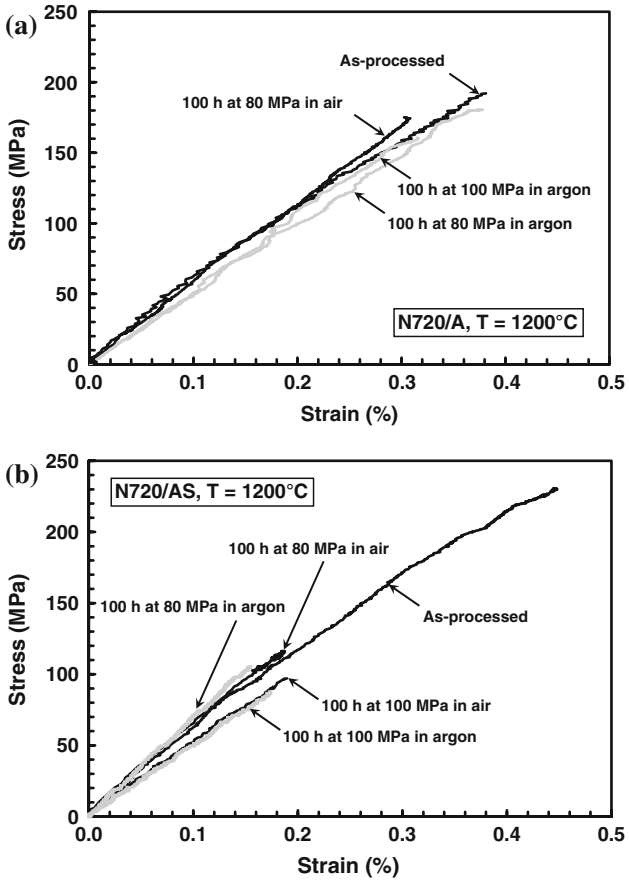

Fig. 7 Effects of prior creep at 1200 °C in laboratory air and in argon on tensile stress–strain behavior of: (**a**) N720/A and (**b**) N720/AS

retained over 83% of their tensile strength, while the modulus loss reached 20%. Conversely, prior creep in air and in argon had a degrading effect on tensile strength of N720/AS. The N720/AS specimens subjected to 100 h of creep in air retained 42% of their tensile strength, whereas the specimens pre-crept in argon retained only 38% of their tensile strength. Prior creep in air or in argon reduced the failure strain of N720/AS by nearly a factor of 3, while modulus loss was limited to 18%.

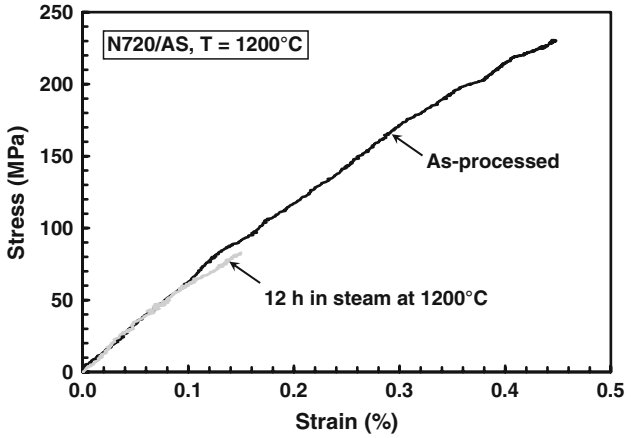

Fig. 8 Effects of 12-h exposure at 1200 °C in steam on tensile stress–strain behavior of N720/AS ceramic composite

The effects of 12-h no-load exposure at 1200 °C in steam on tensile properties of N720/AS are typified in Fig. 8, where a representative stress–strain curve for the aged composite is shown together with the stress–strain curve obtained for the as-processed material. The average tensile strength of the aged specimens was 83 MPa, the average modulus was 70 GPa, and the average failure strain was 0.15%. Short-term aging at 1200 °C in steam resulted in a dramatic 64% loss of tensile strength and a reduction in failure strain by nearly a factor of 3.

Because the creep performance of the composite with 0°/90° fiber orientation is dominated by the fibers, fiber degradation is a likely source of the composite degradation. It is recognized that stress corrosion of the N720 fibers may be the mechanism behind reduced creep resistance of N720/A and N720/AS composites at 1200°C in steam. Earlier studies [26–31] suggested that static fatigue (i.e., delayed fracture under a sustained constant load) of silica-based glasses was a chemical process, where subcritical (slow) crack growth resulted from and was controlled by a stress-enhanced chemical reaction between glass and water in the environment. Michalske and coworkers [32–34] examined the role of mechanical strain in accelerating chemical reactions between the Si–O bonds at the crack tip and environmental molecules and found that the highly strained Si–O bonds reacted with water at least 8 orders of magnitude faster than the unstrained bonds. Michalske and Bunker [34] proposed a quantitative chemical kinetics-based model to predict the rate of crack growth in silica glass in humid condition as a function of the applied stress. This model describes a fracture rate law in which the crack growth rate increases exponentially with the applied stress intensity.

For glass and ceramic materials which have slow crack growth due to stress corrosion as an unique, time-dependent failure mechanism, it is possible to predict the cyclic fatigue lifetime from the static fatigue (creep) data by using a linear elastic crack growth model [35]. Ruggles-Wrenn et al. [36] applied the fracture mechanics approach proposed by Evans and Fuller [35] to the cyclic and static fatigue data obtained for N720/A at 1200 °C in steam. Excellent agreement between predicted cyclic lifetimes and experimental results at 0.1 Hz in steam showed that slow crack growth due to stress corrosion was the governing failure mechanism. However, for the frequencies of 1.0 and 10 Hz and applied stress levels <170 MPa, cyclic lifetimes were underestimated. Improved fatigue durability was attributed to the beneficial effect of progressive matrix cracking, suggesting that matrix plays a considerable role in the overall composite performance.

The results of the present study emphasize the importance of the matrix contribution to the overall composite performance and durability. It is seen that the two composites comprised of the same N720 fibers but two different matrix materials exhibit significantly different behaviors at 1200 °C in steam. Recall that the N720/A and N720/AS composites derive their damage tolerance from porous matrices; therefore, the stability of the matrix porosity against densification is critical to the composite's long-term durability. The loss of matrix porosity would inhibit crack deflection, reduce damage tolerance, and accelerate failure. Reports on the thermal degradation of porous-matrix, oxide/oxide ceramic composite are scarce and somewhat conflicting. Jurf and Butner [23] observed a ~30% decrease in tensile strength of N720/AS composite after 1000 h at 1100 °C in air, while Antti et al. [37] reported that after 100 h at 1100 °C the strength of N720/AS fell to less than one-third of the as-processed strength. Both studies attributed the loss of tensile strength to matrix densification and increased fiber–matrix bonding. Jurf and Butner [23] reported that N720/A composite showed full strength retention after 1000 h at 1200 °C in air. However, Fujita et al. [38, 39] reported that for a composite consisting of Nextel^{TM}720 fibers in a porous alumina matrix, a porosity reduction of ~6% was observed after a 10-min exposure at 1200 °C, which was caused by additional sintering of the matrix. It is likely that N720/A and N720/AS specimens subjected to creep at 1200 °C in steam undergo matrix changes leading to the loss of matrix porosity. Under sustained loading, the loss of matrix porosity and the stress corrosion of the fibers work together to accelerate failure and to reduce lifetime of the composite. Microstructural examination presented below confirms that differences in the response of the alumina and aluminosilicate matrix materials to thermal and environmental exposure under sustained loading are behind the dramatically different creep behaviors of the N720/A and N720/AS composites in steam.

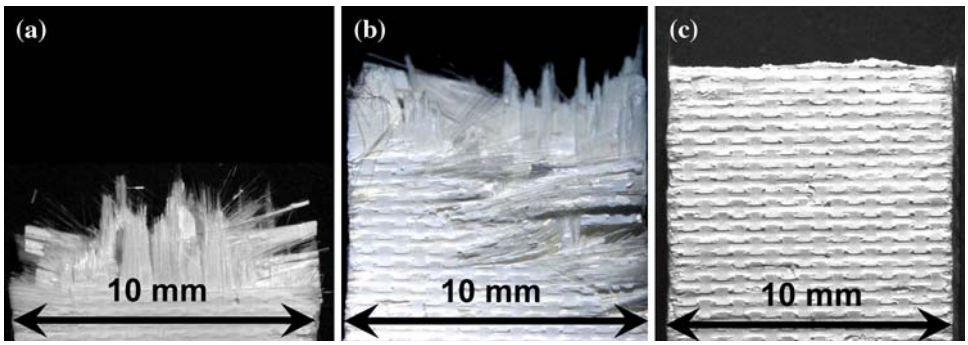

Fig. 9 Fracture surfaces obtained in tensile tests conducted on: (**a**) N720/A as-processed specimen, (**b**) N720/AS as-processed specimen, and (**c**) N720/AS specimen aged at 1200 °C in steam for 12 h

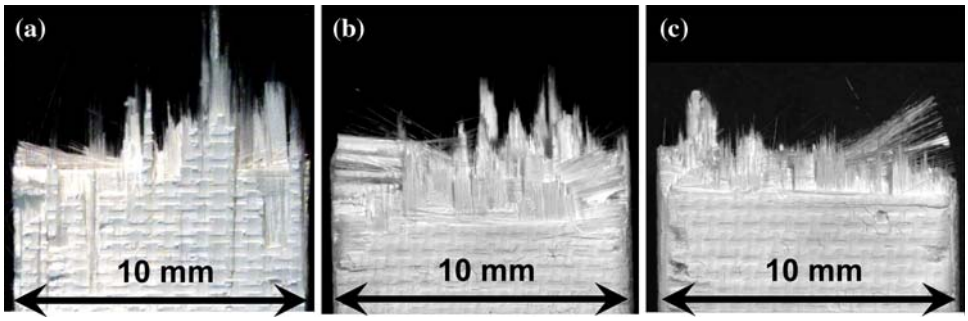

Fig. 10 Fracture surfaces of the N720/A specimens obtained in creep tests conducted at 125 MPa at 1200 °C in: (**a**) argon, $t_f = 36.3$ h; (**b**) air, $t_f = 18.1$ h; and (**c**) steam, $t_f = 0.24$ h

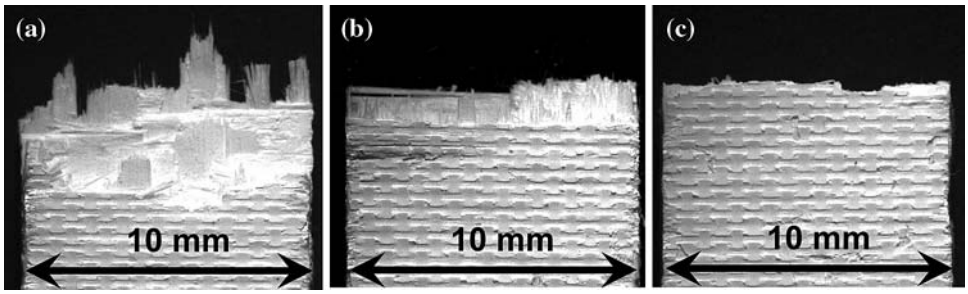

Fig. 11 Fracture surfaces of the N720/AS specimens obtained in creep tests conducted at 125 MPa at 1200 °C in: (**a**) air, $t_f = 30.7$ h; (**b**) argon, $t_f = 1.77$ h; and (**c**) steam, $t_f = 0.2$ h

Composite microstructure

Optical micrographs of fracture surfaces of the as-processed N720/A and N720/AS specimens tested in tension to failure are presented in Fig. 9a and b, respectively. Both composites exhibit damage-tolerant behavior as indicated by fibrous fracture. In contrast, the N720/AS specimen aged for 12 h at 1200 °C in steam (Fig. 9c) produced a nearly flat fracture surface indicative of brittle composite behavior. Note that the N720/AS specimen aged in steam produced an UTS of only 83 MPa, a reduction by nearly a factor of 3 compared to the UTS of 231 MPa obtained for the as-processed specimen.

Optical micrographs of the fracture surfaces obtained in 125 MPa creep tests on N720/A and N720/AS are presented in Figs. 10 and 11, respectively. In general, the fracture surfaces of the N720/A specimens exhibit larger amounts of fiber pullout and longer damage zones than those of the N720/AS specimens. This difference is particularly striking in the case of specimens tested in argon and in steam. The N720/AS fracture surface obtained in argon shows little uncoordinated fiber failure and that obtained in steam exhibits no fibrous fracture at all. On the contrary, the N720/A specimens produced brushy fracture surfaces in all environments. It is seen in Fig. 10 that the N720/A specimen tested in argon, which produced the longest lifetime at 125 MPa ($t_f = 36.3$ h), has a considerably longer damage zone than the N720/A specimens tested in air and in steam. Similar observation can be made regarding the N720/AS fracture surfaces in Fig. 11. The N720/AS specimen tested in air, which exhibited the longest creep lifetime at 125 MPa ($t_f = 30.7$ h) also had the longest damage zone. The N720/A and N720/AS specimens tested in this effort produced damage zones ranging up to 9 mm in length. It is noteworthy that specimens that exhibited longer lifetimes invariably produced longer damage zones.

Further understanding of the influence of environment on the fracture surface topography and the microstructure of N720/A and N720/AS specimens tested in creep at

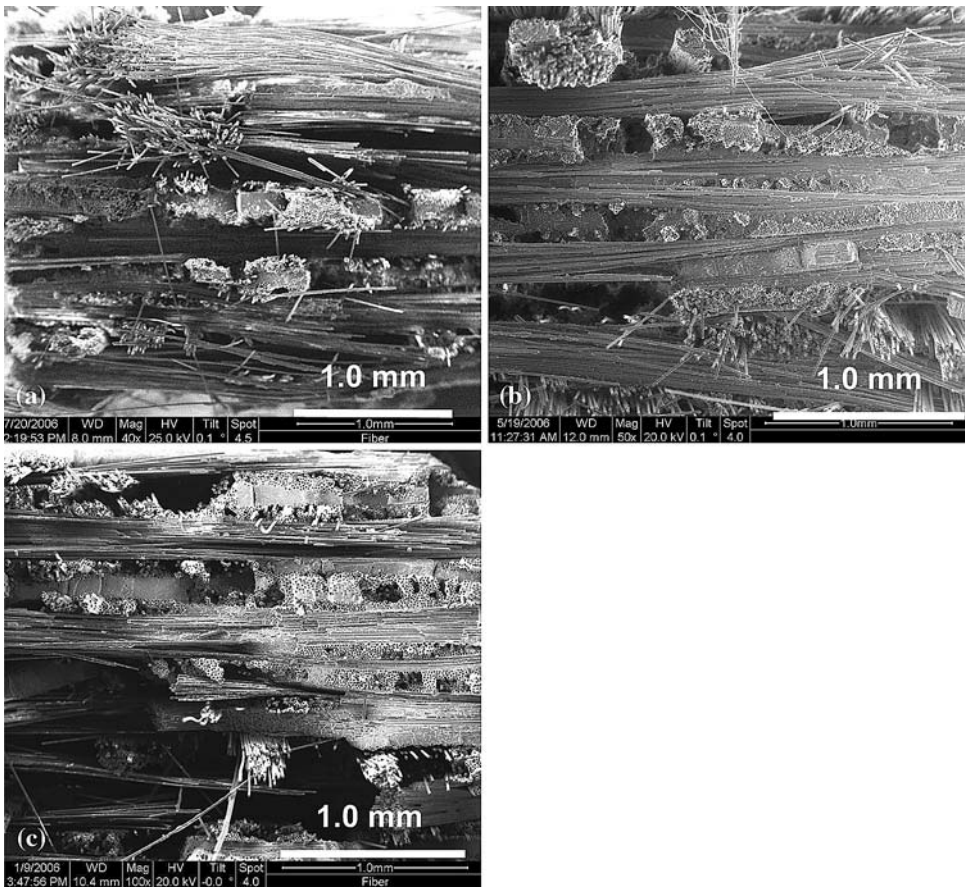

Fig. 12 SEM micrographs of the fracture surfaces of the N720/A specimens obtained in creep tests conducted at 125 MPa at 1200 °C in: (**a**) argon, (**b**) air, and (**c**) steam

125 MPa can be gained by examining SEM micrographs in Figs. 12 and 13. In the case of the N720/A composite, the fracture surface obtained in argon (Fig. 12a) exhibits both regions of nearly planar failure and regions of uncorrelated fiber fracture, where individual fibers are clearly discernable. While the fracture surface produced in air (Fig. 12b) still exhibits some areas of uncoordinated brushy failure, areas of planar fracture become more prevalent. Finally, the fracture surface produced in steam (Fig. 12c) is dominated by planar regions of coordinated fiber failure. Notably, as the extent of correlated fiber failure increases, the creep lifetime decreases. It is recognized that the increase in the spatial correlation in the fiber failure locations is among the main manifestations of the matrix densification [38, 39]. The near-planar fracture surface obtained in steam indicates the loss of matrix porosity and subsequent matrix densification due to additional sintering. As a result, the N720/A composite exhibits decreased damage tolerance and a reduced lifetime.

The fracture surfaces of the N720/AS composite obtained in air (Fig. 13a) and in argon (Fig. 13b) are dominated by areas of planar fracture. The fiber pullout is negligible. The 0° fibers fail in a coordinated fashion, only very short pull-out of sintered bundles can be found. Yet individual 90° fibers are still observed. A dramatically different fracture surface topography is produced in steam (Fig. 13c). The fracture surface is characteristic of brittle failure; the fibers and the matrix break essentially in a coplanar fashion. The material exhibits no fiber pullout, an increased fiber–matrix bonding is apparent. Furthermore, large voids can be seen throughout the fracture surface. A magnified view of a typical void is shown in Fig. 13d. The matrix of the N720/AS composite consists of Al_2O_3 particles bonded together by a continuous SiO_2 film. Matrix porosity comes from incomplete filling of the interparticle voids. The SiO_2 in the matrix is three-dimensionally constrained by the tightly packed Al_2O_3 grains and the surrounding fibers. Under this nearly hydrostatic constraint, thermal exposure leads to coarsening of the pore-size distribution, rather than to the densification of the matrix [40]. Pore coarsening occurs as the regions of high capillary pressure (i.e., small pores) contract and cause larger pores to expand [41]. While the total volume of the composite is constrained dimensionally by the fiber skeleton and cannot change, the smaller matrix pores shrink forcing the larger ones to grow. As a result some matrix regions densify while other dilate forming voids as that seen in Fig. 13d. The coarsening of the porosity of the aluminosilicate matrix and

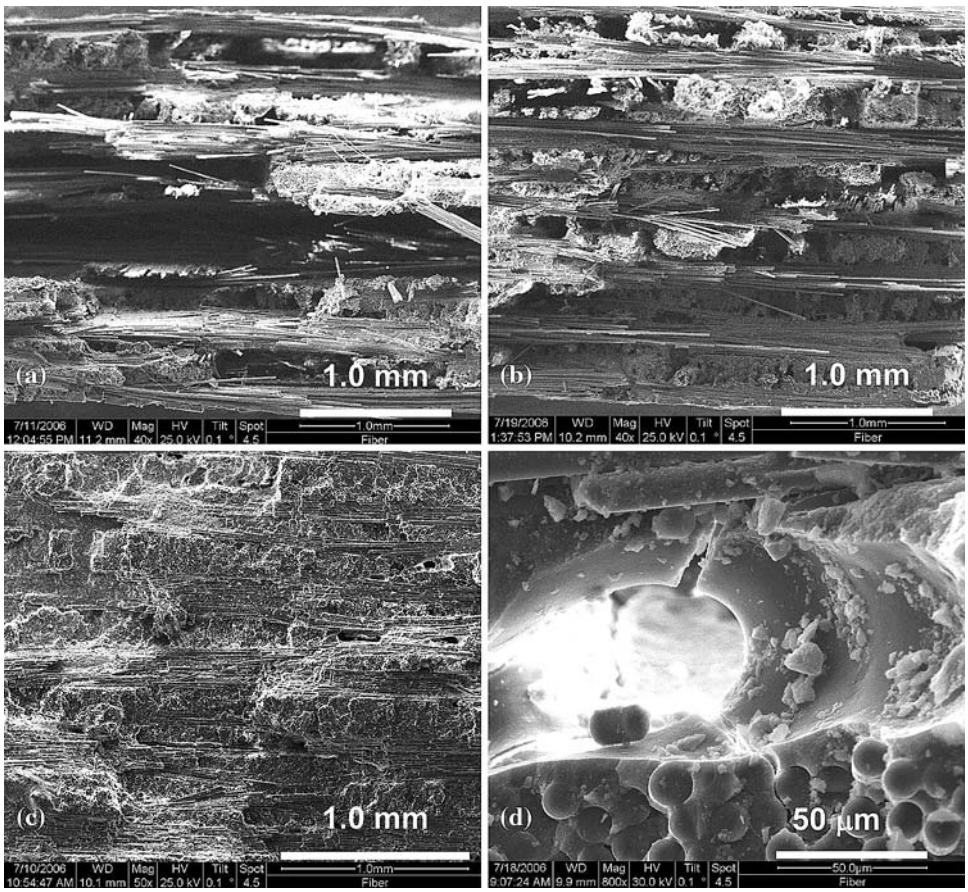

Fig. 13 SEM micrographs of the fracture surfaces of the N720/AS specimens obtained in creep tests conducted at 125 MPa at 1200 °C in: (**a**) air, (**b**) argon, (**c**) steam, and (**d**) steam, showing a matrix void

the increased fiber–matrix bonding inhibit crack deflection, resulting in reduced damage tolerance and poor creep performance of the N720/AS composite in steam.

The fracture surface obtained in a tensile test of the N720/AS specimen aged in steam was also examined and found to be similar to that obtained in the 125 MPa creep test conducted in steam. The fracture surface of the aged specimen also exhibited planar fracture topography with no visible fiber pullout, increased matrix–fiber bonding, and numerous large voids. Apparently, a 12-h no-load exposure in steam at 1200 °C was sufficient to cause coarsening of the porosity in the matrix. As a result, the extent of correlated fiber failure increased and the tensile strength and damage tolerance decreased.

Figures 14 and 15 show the fracture surfaces obtained in tensile tests of the N720/A and N720/AS specimens subjected to 100 h of prior creep at 80 MPa in air and in argon, respectively. Whereas both composites achieved creep run-out at 80 MPa in air and in argon, the retained properties of the two CMCs were very different. The fracture surface of the N720/A run-out specimen tested in air (Fig. 14a, b) exhibits the same general features as the N720/A fracture surface produced in the 125 MPa creep test in air. Conversely, the fracture surface of the N720/AS run-out specimen tested in air (Fig. 14c, d) has the same appearance as the fracture surface of the N720/AS specimen subjected to creep in steam. The near planar fracture surface in Fig. 14c is dominated by areas of coordinated fiber failure and shows increased fiber–matrix bonding. In addition, multiple large voids, as the one shown in Fig. 14d, are also seen. It appears that coarsening of the matrix porosity occurred during the 100 h creep test at 80 MPa in air. The fracture surfaces in Fig. 15 suggest that the same conclusions can be drawn with respect to the N720/A and N720/AS specimens subjected to 100 h of creep at 80 MPa in argon. The fracture surface of the N720/A composite (Fig. 15a, b) shows fairly extensive regions of uncorrelated fiber fracture. This suggests that matrix changes and, consequently, degradation of retained properties were limited. Recall that the N720/A specimen subjected to 100 h of prior creep at 80 MPa in argon retained ~94% of its tensile strength. In contrast, the N720/AS fracture surface in Fig. 15c and d shows planar failure and increased fiber–matrix bonding as well as numerous voids. Apparently 100-h exposure under load at 1200 °C in air or argon causes changes in the matrix akin to those observed after only 12-h no-load exposure in steam or even shorter exposures in steam under sustained loading during creep tests. These

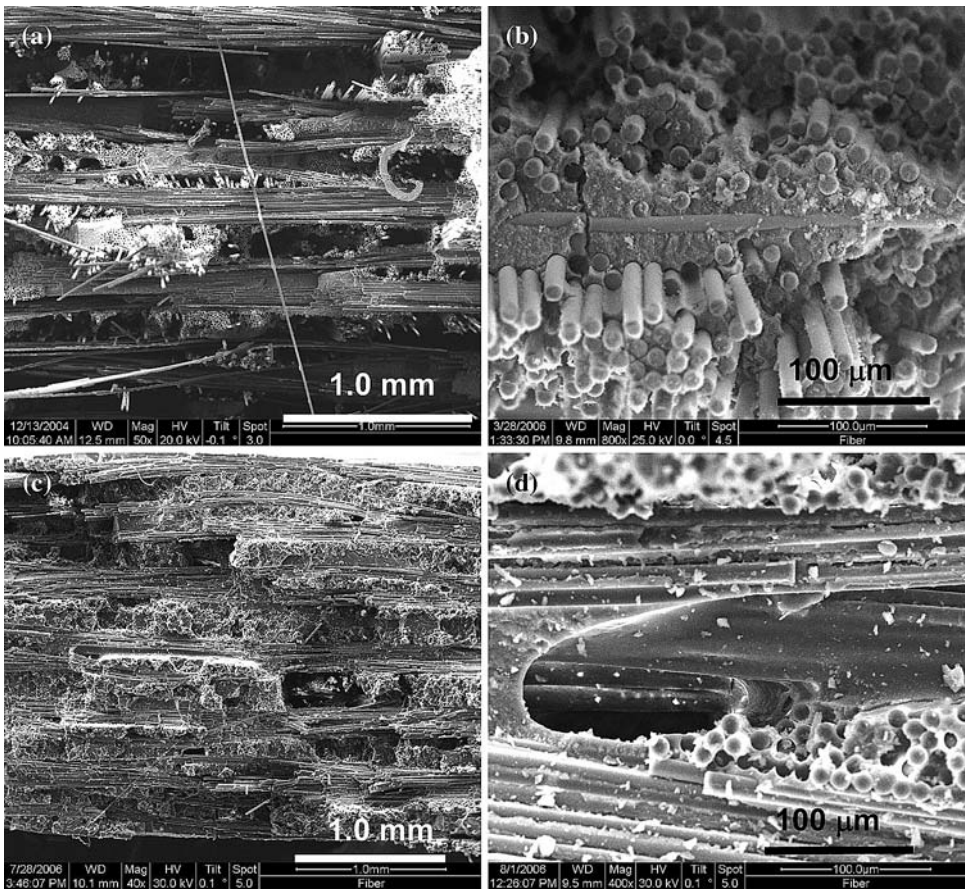

Fig. 14 SEM micrographs of the fracture surfaces obtained in tensile tests conducted on specimens subjected to 100 h of prior creep at 80 MPa at 1200 °C in air: (**a, b**) N720/A and (**c**, **d**) N720/AS

changes in the aluminosilicate matrix lead to considerable loss of tensile strength.

Concluding remarks

The creep–rupture behaviors of the N720/A and N720/AS composites were characterized at 1200 °C in air, steam, and argon environments. The test environment has little influence on the appearance of the creep curves of the N720/A and N720/AS composites. For each composite, the creep curves produced in argon and in steam are qualitatively similar to the creep curves obtained in air. The creep strains accumulated by each composite in argon were comparable to those accumulated in air at a given applied stress. In contrast, creep strains accumulated by each composite at 80 MPa in steam are significantly larger than those produced in air.

Minimum creep rate was reached in all tests. In air, the secondary creep rate of N720/A can be two orders of magnitude higher than that of the N720/AS. The presence of steam accelerates creep rates of N720/A by one order of magnitude and creep rates of N720/AS by nearly two orders of magnitude.

Both composites achieved creep run-out of 100 h at stresses $\leq$100 MPa in air and in argon. Presence of steam dramatically reduced creep lifetimes of both composites. Neither composite achieved creep run-out in steam.

The N720/A fracture surfaces exhibit regions of uncoordinated brushy failure as well as areas of nearly planar fracture. The fracture surface appearance can be correlated with failure time. Predominantly planar fracture surface corresponds to a short life, while fibrous fracture indicates longer life. The N720/AS fracture surfaces produced in tests of <100 h duration conducted in air and in argon show some areas of fibrous fracture. The N720/AS fracture surfaces obtained in tests of $\geq$100 h duration conducted in air and in argon as well as the fracture surfaces obtained in steam exhibit the characteristics of brittle failure.

Stress corrosion of the N720 fibers is likely the mechanism behind poor creep resistance of both N720/A and N720/AS composites in steam. However, the mechanical performance of the N720/AS composite is further degraded by changes in the aluminosilicate matrix, which occur during short-term exposures in steam at 1200 °C as well as during prolonged (>100 h) exposures under sustained load in air and in argon at 1200 °C.

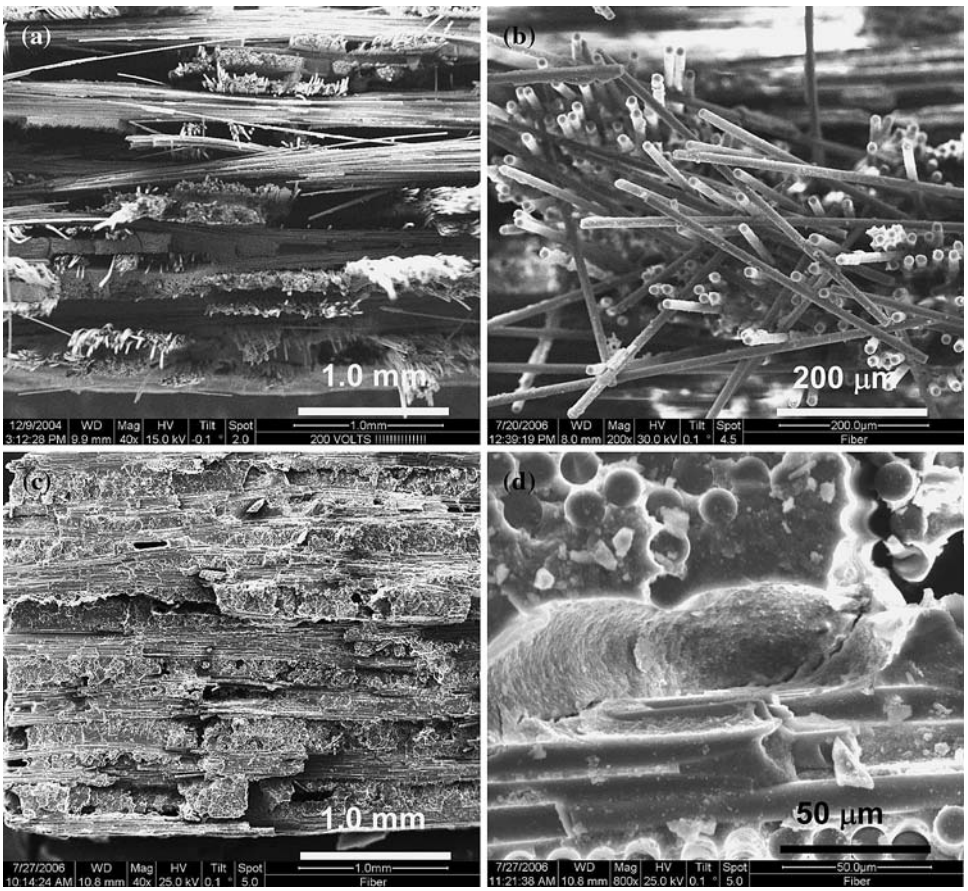

Fig. 15 SEM micrographs of the fracture surfaces obtained in tensile tests conducted on specimens subjected to 100 h of prior creep at 80 MPa at 1200 °C in argon: (**a**, **b**) N720/A and (**c**, **d**) N720/AS

References

1. Ohnabe H, Masaki S, Onozuka M, Miyahara K, Sasa T (1999) Composites Part A 30:489
2. Zawada LP, Staehler J, Steel S (2003) J Am Ceram Soc 86(8):1282
3. Parlier M, Ritti MH (2003) Aerospace Sci Technol 7:211
4. Mattoni MA, Yang JY, Levi CG, Zok FW, Zawada LP (2005) Int J Appl Ceram Technol 2(2):133
5. Parthasarathy TA, Zawada LP, John R, Cinibulk MK, Zelina J (2005) Int J Appl Ceram Technol 2(2):122
6. Szweda A, Millard ML, Harrison MG (1997) Fiber-reinforced ceramic-matrix composite member and method for making. US Patent 5,601,674
7. Sim SM, Kerans RJ (1992) Ceram Eng Sci Proc 13(9–10):632
8. Moore EH, Mah T, Keller KA (1994) Ceram Eng Sci Proc 15(4):113
9. Lange FF, Tu WC, Evans AG (1995) Mater Sci Eng A 195:145
10. Mouchon E, Colomban P (1995) Composites 26:175
11. Tu WC, Lange FF, Evans AG (1996) J Am Ceram Soc 79(2):417
12. Evans AG, Zok FW (1994) J Mater Sci 29:3857
13. Kerans RJ, Parthasarathy TA (1999) Composites Part A 30:521
14. Kerans RJ, Hay RS, Parthasarathy TA, Cinibulk MK (2002) J Am Ceram Soc 85(11):2599
15. Levi CG, Yang JY, Dalgleish BJ, Zok FW, Evans AG (1998) J Am Ceram Soc 81:2077
16. Hegedus AG (1991) Ceramic bodies of controlled porosity and process for making same. U.S. Patent 5,0177,522
17. Lu TJ (1996) J Am Ceram Soc 79:266
18. Zok FW, Levi CG (2001) Adv Eng Mater 3(1–2):15
19. Zok FW (2006) J Am Ceram Soc 89(11):3309
20. Lee SS, Zawada LP, Staehler J, Folsom CA (1998) J Am Ceram Soc 81(7):1797
21. Zawada LP, Hay RS, Lee SS, Staehler J (2003) J Am Ceram Soc 86(6):981
22. Ruggles-Wrenn MB, Mall S, Eber CA, Harlan LB (2006) Composites Part A 37(11):2029
23. Jurf RA, Butner SC (1999) Trans ASME J Eng Gas Turbines Power 122(2):202
24. Staehler JM, Zawada LM (2000) J Am Ceram Soc 83(7):1727
25. Szymczak N (2007) MS Thesis. Air Force Institute of Technology, WPAFB, OH
26. Charles RJ, Hillig WB (1962) In: Symposium on mechanical strength of glass and ways of improving it. Union Scientifique Continentale du Verre, Belgium, p 511
27. Charles RJ, Hillig WB (1965) In: Zackey VF (ed) High-strength materials. Wiley, New York, p 682
28. Wiederhorn SM (1967) J Am Ceram Soc 50(8):407
29. Wiederhorn SM, Bolz LH (1970) J Am Ceram Soc 53(10):543
30. Wiederhorn S (1972) J Am Ceram Soc 55(2):81
31. Wiederhorn SM, Freiman SW, Fuller ER, Simmons CJ (1982) J Mater Sci 17:3460
32. Michalske TA, Freiman SW (1983) J Am Ceram Soc 66(4):284
33. Michalske TA, Bunker BC (1984) J Appl Phys 56(10):2686
34. Michalske TA, Bunker BC (1993) J Am Ceram Soc 76(10):2613
35. Evans AG, Fuller ER (1974) Metall Trans A 5(1):27

36. Ruggles-Wrenn MB, Hetrick G, Baek SS (2007) Int J Fatigue, in press
37. Antti ML, Lara-Curzio E, Warren R (2004) J Eur Ceram Soc 24:565
38. Fujita H, Jefferson G, McMeeking RM, Zok FW (2004) J Am Ceram Soc 87(2):261
39. Fujita H, Levi CG, Zok FW, Jefferson G (2005) J Am Ceram Soc 88(2):367
40. Sherer GW (1998) J Am Ceram Soc 81(1):49
41. Bordia RK, Jagota A (1993) J Am Ceram Soc 76(10):2475